Optical investigation of a strain-induced mixed type-I–type-II superlattice system: $CdTe/Cd_{1-x}Zn_xTe$

H. Tuffigo and N. Magnea
Département de Recherche Fondamentale, Service de Physique,
Groupe Physique des Semiconducteurs,
Centre d'Etudes Nucléaires de Grenoble, Boîte Postale No. 85X, 38041 Grenoble CEDEX, France

H. Mariette, A. Wasiela, and Y. Merle d'Aubigné
Laboratoire de Spectrométrie Physique, Université Joseph Fourier, Boîte Postale 87X, 38042 Grenoble CEDEX, France
(Received 30 April 1990; revised manuscript received 3 December 1990)

We present a systematic optical study of strained, $CdTe/Cd_{1-x}Zn_xTe$ ($x \approx 0.1$) superlattices grown by molecular-beam epitaxy. We have observed the intrinsic heavy- and light-hole exciton transitions of these superlattices, as well as the excited states ($2s$) of the heavy-hole exciton. By studying the energy variation of these transitions as a function of the period, we point out the mixed nature of the superlattice band structure (type I or II for heavy- or light-hole exciton transitions, respectively) due to the opposite strain experienced by the two kinds of layer (CdTe and $Cd_{1-x}Zn_xTe$); this is revealed by the relative variation of the light-hole exciton binding energy as a function of the superlattice period compared with that of the heavy hole. All these data provide a determination of the partition of the band-gap discontinuities between the valence and the conduction bands, found to lie between 1/9 and $-1/11$. Because the valence-band configuration is essentially influenced by the strain, we change the respective energy positions of the direct and indirect exciton transitions just by changing the average strain in the superlattice (namely, by growing the structures on buffer layers of different zinc concentrations); therefore we observe a strain-mediated type-I–type-II transition.

I. INTRODUCTION

In the past few years, strained-layer superlattices, especially systems made with III-V materials,[1–3] have received increasingly intensive study. These structures consist of alternating layers of two lattice-mismatched materials A and B. Provided that the layer thicknesses are less than some strain-dependent critical values, the mismatch is accommodated by elastic strain rather than by misfit dislocations at the interface (the "critical thickness" is defined as the thickness beyond which the misfit strain relaxes).

In this paper, we discuss remarkable features observed in a II-VI strained-layer superlattice (SLS) system characterized by a very small valence-band offset in the absence of strain. In such a situation, strain does much more than just perturb the band structure; instead, it totally governs the valence subbands of the superlattice. In particular, one can expect the following.

(i) The superlattice will be an unusual, mixed type system:[4] type I for heavy-hole excitons (the electrons and holes being confined in the same material A) and type II for light-hole excitons (the electrons and the light holes being confined in materials A and B, respectively, that is, the light-hole exciton will be "indirect"[5] in real space).

(ii) The relative energy position of the type-I and the type-II excitons can be *inverted* simply by changing the superlattice strain state using different buffer layers, a particularly interesting illustration of "band-gap engineering" (the SLS is then designated type I or II depending on which exciton is lowest).

These properties are illustrated here for the $CdTe/Cd_{1-x}Zn_xTe$ system by performing a systematic spectroscopic study: reflectivity, photoluminescence (PL), photoluminescence excitation (PLE), and optical-pumping experiments lead to a clear identification of the optical transitions of the heavy- and light-hole excitons of the SLS's and show the strong influence of the strain on the type of the superlattice.

For superlattices based on Cd and Zn tellurides, most of the reported work concerns *free-standing* SLS's (i.e., superlattices relaxed to their own lattice parameter instead of maintaining the lattice constant of the buffer layer) built from the two *binary* compounds.[6,7] However, due to the large lattice mismatch between CdTe and ZnTe (6.4%), only short period SLS's can be grown [the critical thickness of CdTe on ZnTe is 17 Å (Ref. 8)]. Moreover, the dislocations that appear in such samples degrade the optical spectra—in particular, the excitonic transitions are broad, typically ≥ 10 meV wide.[7]

By contrast, the specificity of the samples studied here is as follows: (i) they are built from CdTe and Cd-rich $Cd_{1-x}Zn_xTe$ *ternary* alloy with $x \approx 10\%$; the critical thickness related to the small misfit ($\approx 0.6\%$) between the two kinds of layers is now as large as 1000 Å; (ii) the whole superlattice can be grown *coherently* with the substrate or the buffer layer (i.e., having the same in-plane lattice parameter).

Photoluminescence excitation spectroscopy is used to study the evolution of the electronic states and their associated optical transitions as a function of the SLS band structure. Strong and sharp excitonic resonances are observed. We show the mixed nature of the SLS band-gap configuration: electrons and heavy holes are confined in the CdTe layers (type I or direct transition) whereas light holes are confined in $Cd_{1-x}Zn_xTe$ barriers (type II or indirect transition). This peculiar band structure leads to the observation of two effects. First, the dependence of the exciton binding energy on the SLS period is different for direct and indirect transitions. Secondly, by modifying the strain in the SLS we can change the respective positions of the direct and indirect transition lines and, therefore, observe the strain-mediated type-I–type-II passage.

This paper is organized in the following way: in Sec. II, we describe briefly the sample growth and the strain characteristics of the superlattices presented here. In Sec. III, we detail the spectroscopic results that are obtained on such superlattices and the interpretation of these optical data. Section IV is devoted to the influence of the superlattice period on these optical properties. Section V presents the observation of the excitonic excited states that allow one to determine the exciton binding energies and to evaluate (Sec. VI) the valence-band offset of this system. Finally, in Sec. VII, the influence of the average strain in such superlattices is probed by comparing the optical properties of samples grown on different buffer layers; in particular, we show how it is possible to change the band structure from a type-I superlattice to a type-II superlattice just by adjusting the strain induced on the superlattice by the buffer layer. Our results are summarized in the conclusion.

II. EXPERIMENT

The samples are grown by molecular-beam epitaxy in a Riber 32P machine on {001}-oriented $Cd_{1-y}Zn_yTe$ ($y \approx 0.04$) substrates.[9] Reflection high-energy electron diffraction provides the means to optimize the two-dimensional layer-by-layer growth of CdTe and $Cd_{1-x}Zn_xTe$ alloy and to measure the layer thickness *in situ* to one monolayer accuracy; the alloy composition x together with the superlattice period are precisely determined from x-ray data.[10] The samples discussed in this paper consist of *equal-thickness* layers of CdTe and $Cd_{1-x}Zn_xTe$ (with the amount of zinc ranging between 6% and 12%). They are grown either directly on CdTe or $Cd_{1-x}Zn_xTe$ ($x \approx 0.04$) substrates or on a buffer layer, which is either CdTe or $Cd_{1-x}Zn_xTe$ ($x \approx 0.08$). In this way, we tune the biaxial compression present in the CdTe layers of the superlattice and the biaxial dilatation experienced by the $Cd_{1-x}Zn_xTe$ ($x \approx 0.08$) layers. For SLS's grown $Cd_{1-x}Zn_xTe$ ($x \approx 0.04$), the strains in the CdTe and the $Cd_{1-x}Zn_xTe$ ($x \approx 0.08$) layers are equal and opposite, which corresponds to the concept of strain symmetrization developed for Si/Ge SLS systems.[11]

The different spectroscopic techniques and the experimental details used in this work are described in Refs. 12 and 13.

III. GENERAL RESULTS

Figure 1 presents optical spectra obtained for sample S1 [period (130 Å)/(130 Å), grown directly on the $Cd_{1-x}Zn_xTe$ ($x \approx 0.04$) substrate]. The PL spectrum is

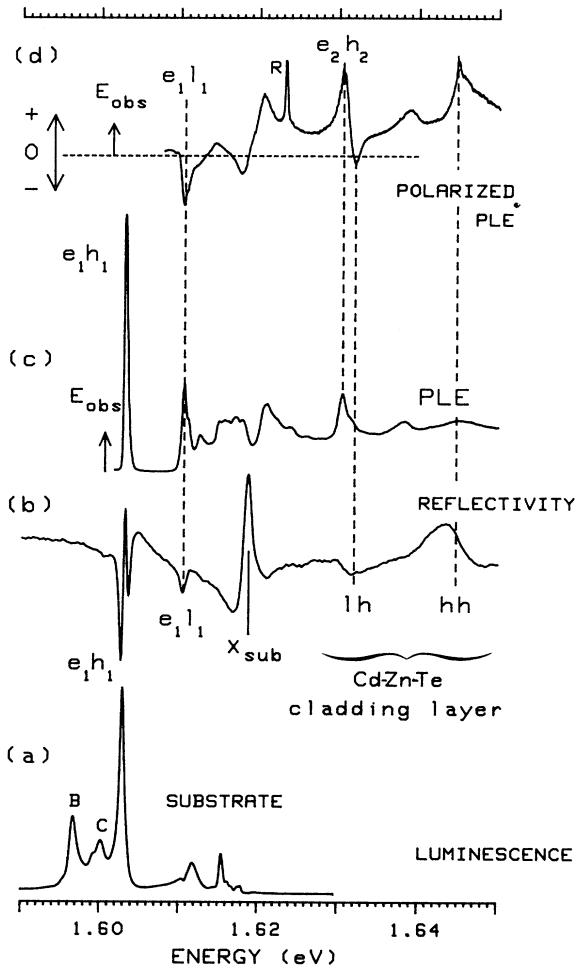

FIG. 1. Optical spectra obtained at 1.8 K for a $CdTe/Cd_{1-x}Zn_xTe$ ($x \approx 0.08$) superlattice consisting of ten (130 Å)/(130 Å) periods (sample S1). (a) Photoluminescence spectrum showing the intrinsic heavy-hole exciton line e_1h_1 and extrinsic lines B and C, as well as substrate donor- and acceptor-bound exciton lines. (b) Reflectivity spectrum showing both SLS excitonic ground states e_1h_1 and e_1l_1. Label X_{sub} designates the sustrate's free exciton; *lh* and *hh* are the strain-split, light- and heavy-hole excitons in the $Cd_{1-x}Zn_xTe$ ($x \approx 0.08$) cladding layer. (c) Excitation spectrum of line C: besides the e_1h_1 and e_1l_1 lines, the e_2h_2 exciton is clearly identifiable in agreement with the calculation; R is a Raman line. (d) Circular polarization of the e_1h_1 emission as a function of excitation wavelength, for σ_+ excitation. The negative polarization signals associated with light-hole contributions correspond to, successively, the superlattice transition e_1l_1, a $Cd_{1-x}Zn_xTe$-substrate contribution (1.618 eV), and cladding-layer transition *lh*.

dominated by a line labeled e_1h_1 at 1602.9 meV, which corresponds to the recombination of the heavy-hole exciton of the SLS. The high intensity of this transition in the reflectivity spectrum [Fig. 1(b)] and the PLE spectrum [Fig. 1(c)], as well as in transmission spectra,[10] is a strong indication that this transition is both intrinsic and direct (i.e., type I). At lower energy in the PL spectrum, we observe two lines, labeled B and C; these lines do not appear in reflectivity [Fig. 1(d)] so they represent a low density of states and are attributed to excitons trapped by impurities or interface defects. Indeed, these lines are strongly reminiscent of the acceptor and donor bound exciton (A^0X and D^0X) transitions observed in $Cd_{0.96}Zn_{0.04}Te$ alloys. Their energy positions as well as their unequal broadening due to alloy fluctuations (larger for A^0X than for D^0X) are comparable to what is obtained in bulk alloys.[14]

The excitation spectrum monitored on line C [Fig. 1(c)] clearly shows, beside the feature corresponding to the intrinsic e_1h_1 exciton of the superlattice, a second peak, labeled e_1l_1, at higher energy (1611 meV); the latter transition is also seen in reflectivity [Fig. 1(b)] with a lower intensity than e_1h_1. To deduce the light- or heavy-hole character of this excitonic transition, optical-pumping experiments were performed. In this technique[15] one excites with circularly polarized light (σ^+ in our case) at different wavelengths and one measures the circular polarization of the emission. If the excitation and the emission transitions have the same character (i.e., both involving heavy-hole excitons or both involving light-hole excitons), the measured circular polarization is positive; if they have different characters (i.e., one with heavy hole and the other with light hole) this polarization is negative. The polarized excitation spectrum of Fig. 1(d), monitored on the heavy-hole exciton line e_1h_1, shows that the transition e_1l_1 has opposite polarization to e_1h_1. This clearly demonstrates the light-hole character of the transition e_1l_1.

We have always observed (for the whole series of samples studied) a negative polarization at an energy slightly lower than the substrate 1s transition. This is not fully understood yet, but might be explained by a lifting of the valence-band degeneracy due to a strain experienced by several monolayers of the substrate at the superlattice-substrate interface; or it might be explained by a contribution of extrinsic transitions (excitons bound to residual donors), for which the polarization is not well defined. The third negative feature observed in this spectrum (at 1632 meV) corresponds to the light-hole exciton of the strained $Cd_{1-x}Zn_xTe$ cladding layer grown at the top of the superlattice.

The calculated band-structure configuration of these superlattices shows that the light holes are mainly confined in the $Cd_{1-x}Zn_xTe$ layers (whereas electrons and heavy holes are mainly confined in the CdTe layers). The assignment of the observed SLS transitions e_1h_1, e_1l_1, and e_2h_2 (Fig. 1) is consistent with a Kronig-Penney calculation assuming that the valence-band offset is zero in the absence of strain, and using $m_e=0.099m_0$ and $m_{hh}=0.513m_0$, $m_{lh}=0.156m_0$ for the effective masses in CdTe.[16] We account for the strain as in Ref. 17, using the pressure coefficient values found for these samples from the luminescence pressure dependence under a diamond-anvil cell[18] (the partition coefficient of the hydrostatic deformation potential between the conduction and valence bands being given by Camphausen, Connel, and Paul[19]). Then the differences between the calculated band gaps and the experimental positions of the e_1h_1 and the e_1l_1 excitonic transitions give us an estimate of the binding energy of the heavy-hole exciton (14 meV) and light-hole exciton (4 meV). The first value is in good agreement with the value of the exciton binding energy (13 meV) deduced from the 2s-1s difference for a similar superlattice sample where the 2s state was identified through its diamagnetic shift.[20] The smaller value for the light-hole binding energy appears reasonable for an indirect exciton. However, due to the small confinement potentials of the system, the probability of finding an electron or a light hole in their respective barriers is not negligible ($\approx 10\%$ for the sample we are discussing); this gives a ratio of 0.3 between the overlap integrals of the light-hole transition and the heavy-hole one. Taking into account the additional factor of 3 due to the optical dipole matrix elements, we obtain a factor of ≈ 0.1 between the oscillator strength of the two transitions in qualitative agreement with what is observed experimentally in transmission spectra.[10]

Note that trying to attribute the e_1l_1 transition to a direct exciton recombination—with electrons and light holes confined in the CdTe layers—would require a (strain-free) valence-band offset α of at least 40%, in order to compensate for the effect of the strain on the shape of the potential; α (also called the chemical valence-band offset) is defined as $\Delta E_v/\Delta E_g$ where ΔE_v is the valence-band potential *in the absence of strain* and ΔE_g is the band-gap difference. This attribution would lead to a value of the heavy-hole exciton binding energy lower than the 3D rydberg. Moreover, such a value of the valence-band offset would lead to binding energies for the heavy-hole exciton smaller than for the light-hole exciton; this is not consistent with the fact that even in this potential configuration (with the ground state for the light holes in the CdTe layers) the light holes are quite delocalized between CdTe and $Cd_{1-x}Zn_xTe$, and then the e_1l_1 exciton binding energy has to be much lower than the e_1h_1 one. Consequently, this hypothesis of a large valence-band offset is not valid and, therefore, all the data presented in this paper will be interpreted assuming that the whole band-gap difference lies in the conduction band in the absence of strain (e.g., $\alpha=0$); then, the electrons and heavy holes are confined in the CdTe layers whereas the light holes are confined in the $Cd_{1-x}Zn_xTe$ layers. We will describe in Sec. V the procedure to obtain lower and upper limits for the parameter α from our experimental results.

Figure 2 compares the same series of spectra (PL, reflectivity, PLE, polarized PLE) obtained for sample S2, a (200 Å)/(200 Å) $CdTe/Cd_{0.92}Zn_{0.08}Te$ superlattice grown on a $Cd_{0.96}Zn_{0.04}Te$ substrate. A superlattice of such a period can be considered in a first approximation

as a multiple quantum well with no coupling between adjacent wells. These spectra look very similar to those for sample S1. The two low-energy lines (labeled *B* and *C*) observed in photoluminescence correspond to extrinsic states, as in the previous case, since they are not observed in the reflectivity spectrum. The light indirect e_1l_1 transition at 1607.2 meV is identified because of its negative sign in the polarized photoluminescence excitation spectrum. At higher energy, the PLE spectrum is less resolved than in the case of sample S1 but the reflectivity spectrum allows identification of the 1*s* transition of the substrate, as well as the light- and heavy-hole transitions related to the cladding layer. The main difference between the two samples S1 and S2 is the presence of the lines that we have attributed to "forbidden" exciton states e_1h_2, e_1h_3 in the figure representing spectra for sample S2; we mention that at this well thickness ($L \approx 200$ Å), one may also use an alternative description, assigning these lines to the $N=2$ and 3 quantized states of the exciton center-of-mass motion in the CdTe layers[21] (since the passage from the quantization of the center-of-mass motion to separate carrier quantization is expected to occur at about this well thickness[22]).

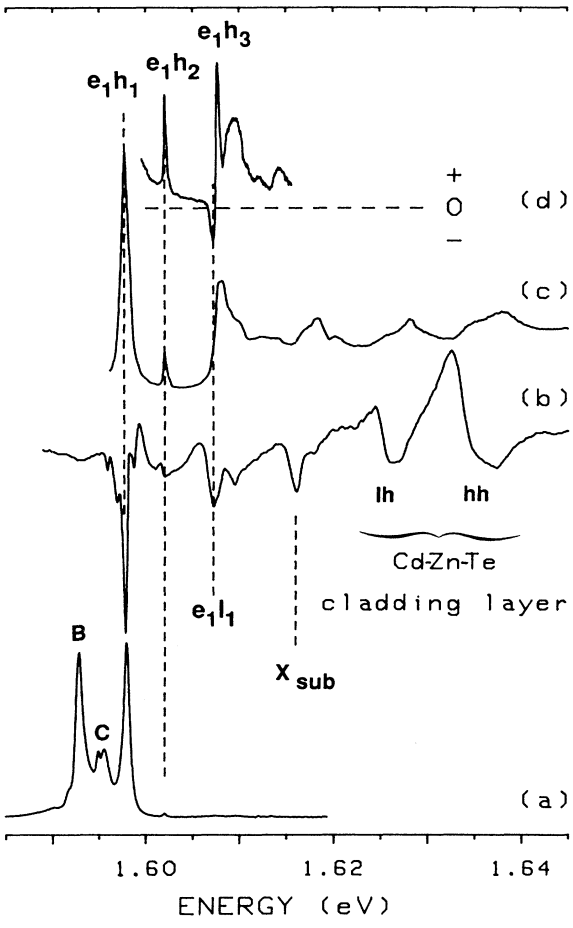

FIG. 2. Optical spectra obtained at 1.8 K for a $CdTe/Cd_{1-x}Zn_xTe$ ($x \approx 0.08$) for superlattice consisting of 20 (200 Å)/(200 Å) periods (sample S2). (a) Photoluminesence spectrum showing the intrinsic e_1h_1 exciton line and extrinsic lines *B* and *C*. (b) Reflectivity spectrum showing the excitonic states e_1h_1, e_1h_2, e_1h_3, the light-hole exciton e_1l_1, the 1*s* exciton of the substrate, as well as the light- and heavy-hole excitons of the cladding layer. (c) PLE spectrum detected at the energy of the intrinsic e_1h_1 exciton. (d) Polarized PLE spectrum allowing identification the light-hole e_1l_1 exciton at 1607.2 meV (corresponding to a negative signal) among the other features of the spectrum such as the e_1h_2 and e_1h_3 exciton states.

IV. INFLUENCE OF THE PERIOD

Figure 3 compares the PL spectra obtained for four superlattices with period ranging between 121 and 400 Å with well and barrier of equal thicknesses; the arrows show the energy positions of the heavy-hole (e_1h_1) and light-hole (e_1l_1) excitons, whereas the dashed straight line is plotted at the energy of the 1*s* exciton of the $Cd_{1-x}Zn_xTe$ alloy equivalent to the average superlattice of the series (that is the limit of the superlattice when the period goes to zero). The whole series of spectra look very similar showing for every sample the extrinsic lines (*B* and *C*) as well as the intrinsic heavy-hole exciton line (e_1h_1). The structure observed in the e_1h_1 line is not clearly explained yet; it could be due to reabsorption or a polariton effect. The indirect light-hole exciton line (e_1l_1) appears in the PL spectra only for the shorter-period superlattices; for the other superlattices, the e_1l_1 line has been observed in the PLE spectra (see the two dashed spectra in Fig. 3) and identified by comparing the relative oscillator strengths in the reflectivity spectra and by performing optical-pumping measurements. Due to confinement effects, the whole superlattice emission shifts towards higher energy as the period decreases. Moreover, one can clearly see that the superlattice emission tends towards the energy of the 1*s* exciton of the alloy equivalent to the superlattice.

We have plotted in Fig. 4 the experimental energy positions of the e_1h_1 and e_1l_1 excitonic transitions as a function of the period of the superlattice. The thin, continuous and dashed lines represent the variations of the optical gaps $E_{E_1H_1}$ and $E_{E_1L_1}$, respectively, obtained using the same calculation as before. Note that for this paper, we use upper-case symbols E_1H_1, etc., to represent optical gaps and lower-case symbols e_1h_1, etc., to represent the corresponding excitons. The heavy-hole exciton energy $E_{e_1h_1}$ follows the optical gap $E_{E_1H_1}$ as the period increases, which shows that, over this range of thickness, the heavy-hole exciton binding energy (of the order of 14 meV, i.e., only 40% larger than in bulk CdTe) remains roughly constant. The experimental values of the light-hole exciton binding energies (i.e., the energy difference between the experimental excitonic energies and the calculated optical gaps, see Fig. 4) are always smaller than the heavy-hole exciton values, which appears reasonable for an indirect exciton. Moreover, the energy position of e_1l_1 tends towards the calculated optical gap $E_{E_1L_1}$ as the period increases; in other words, the light-hole exciton binding energy decreases drastically when the period increases. This result is fully consistent

with the indirect nature of the light-hole exciton; the larger the period, the smaller the overlap integral, and therefore, the smaller the indirect exciton binding energy.

To verify this interpretation of our experimental results, we have calculated the ratio between the overlap of the electron and hole envelope functions (over one period) for the case of light and heavy holes, respectively.[23] We obtain a ratio of 0.3 in the case of a (140 Å)/(140 Å) $CdTe/Cd_{0.92}Zn_{0.08}Te$ superlattice and of 0.9 in the case of a (70 Å)/(70 Å) $CdTe/Cd_{0.92}Zn_{0.08}Te$ superlattice. These surprisingly large values are due to the small band discontinuities of this system: the probability of finding an electron or a light hole in their respective barriers is indeed not negligible [10% for a (140 Å)/(140 Å) superlattice]. The relative variation of the ratio [see Fig. 4(b)] shows the effect of the confinement on the localization of the carriers in their respective wells: in the case of short-period superlattices, the light-hole exciton is "less indirect." This partially explains why in the luminescence spectra the indirect light-hole exciton appears much more clearly for the short-period superlattices (see Fig. 3).

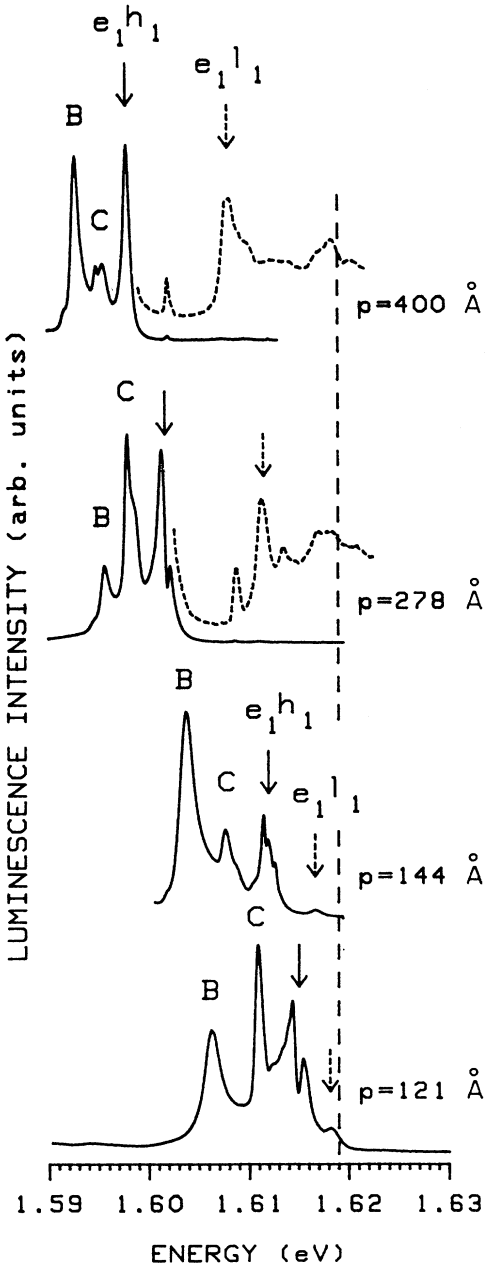

FIG. 3. Photoluminesence spectra (solid line) and photoluminescence excitation spectra (dotted line) obtained for four $CdTe/Cd_{1-x}Zn_xTe$ ($x \approx 0.08$, $L_{CdTe} = L_{Cd_{1-x}Zn_xTe}$) SLS's with periods ranging from 121 to 400 Å. The spectra show the extrinsic lines *B* and *C*, as well as the intrinsic heavy- (e_1h_1, solid arrow) and light- (e_1l_1, dotted arrow) hole exciton lines. The confinement induces a shift of the whole spectrum towards higher energies as the period decreases. The dashed straight line shows the energy of the free exciton in the alloy that is equivalent to the average superlattice of the series (limit when the SLS period tends to zero).

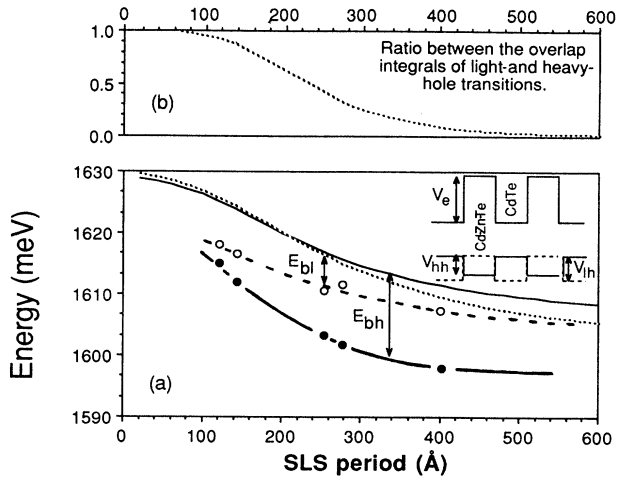

FIG 4. (a) Influence of the SLS period on the calculated gaps $E_{E_1H_1}$ (thin solid line) and $E_{E_1L_1}$ (thin dashed line) for $CdTe/Cd_{1-x}Zn_xTe$ SLS ($x \approx 0.08$, $L_{CdTe} = L_{Cd_{1-x}Zn_xTe}$, grown on a $Cd_{0.96}Zn_{0.04}Te$ substrate) and on the experimental excitonic energies $E_{e_1h_1}$(●) and $E_{e_1l_1}$(○) for samples presented in Figs. 1, 2, and 3 (the thick solid and dashed lines drawn through the experimental points are only a guide for the eye). The inset represents the schematic band structure of the SLS. (b) Influence of the SLS period on the ratio between the overlap integral of electron and light-hole, and of electron and heavy-hole, wave functions.

V. OBSERVATION OF THE EXCITED STATES

Figure 5 shows the luminescence spectrum obtained for sample S3 [(70 Å)/(70 Å) $CdTe/Cd_{0.92}Zn_{0.08}Te$] where the *B* and *C* extrinsic lines as well as the e_1h_1 heavy-hole exciton line (1612.0 meV) are identified as explained in Sec. II for sample S1 or sample S2. The luminescence excitation spectrum detected on line *C* shows the e_1h_1 line. At higher energy (1616.6 meV) the e_1l_1 light-hole excitonic transition has been identified by comparison with the polarized photoluminescence excitation spectrum

(this transition is also observed in photoluminescence). Finally, at still higher energy, there appears a series of lines that have been attributed to the excited states of the e_1h_1 exciton through their behavior as a function of a magnetic field applied perpendicular to the layers.[20] The Zeeman effect induces a diamagnetic shift on the excitonic transitions that should be much more pronounced for the excited states than for the ground state ($1s$) of the exciton. It is shown experimentally[20] that the shift of the line observed at 1621.6 meV (at zero field) as a function of the magnetic field is indeed consistent with the shift predicted for the $2s$ exciton state. This result provides therefore an unambiguous identification of the $2s$ state of the e_1h_1 exciton.

Since the $2s$-$1s$ energy separation (9.8 meV) is not very different from the value in the bulk ($11\times3/4\approx8.2$ meV), one can obtain a good approximation of the exciton binding energy and consequently of the optical gap $E_{E_1H_1}$ through the following expression:

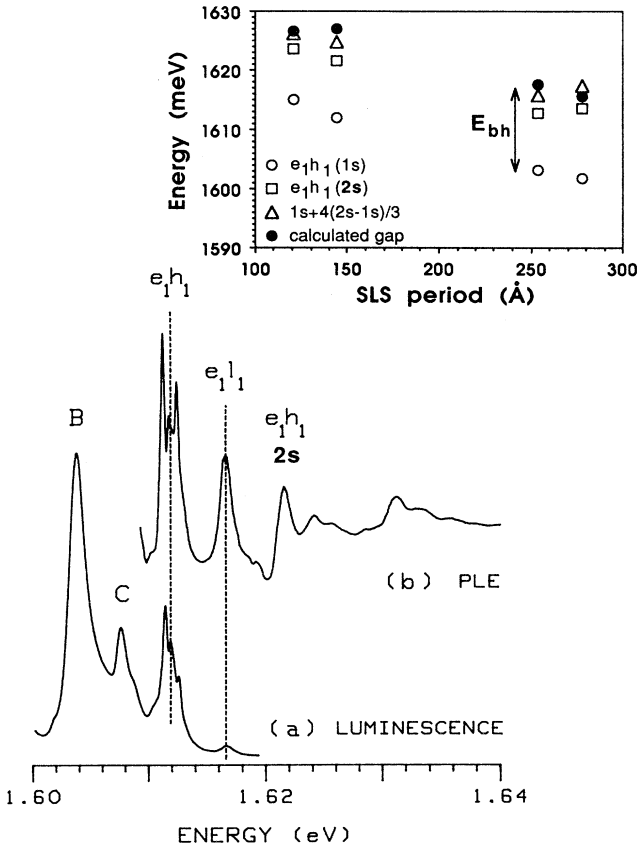

FIG. 5. (a) Photoluminescence spectrum of sample S3, a (70 Å)/(70 Å) $CdTe/Cd_{0.92}Zn_{0.08}Te$ superlattice showing the extrinsic lines B and C as well as the intrinsic e_1h_1 and e_1l_1 exciton lines. (b) PLE spectrum detected on line C showing the intrinsic e_1h_1 and e_1l_1 exciton lines as well as the $2s$ excited state of the e_1h_1 exciton. The inset compares the energy positions of the experimental optical gap (△) obtained using the $2s$-$1s$ energy difference and the calculated gap (●) for superlattice samples with various periods.

$$E_{E_1H_1}=E_{e_1h_1(1s)}+\tfrac{4}{3}[E_{e_1h_1(2s)}-E_{e_1h_1(1s)}]\ .$$

We have obtained values of the $E_{E_1H_1}$ optical gap for four different samples for which we have experimentally observed the $2s$ excited state of the e_1h_1 exciton line; the inset of Fig. 5 compares these values (△) with the calculated values (●) of $E_{E_1H_1}$ (obtained using the same Kronig-Penney model as previously with $\alpha=0$). The good agreement between the values $E_{E_1H_1}$ obtained in two different ways is a second proof of the identification of the $2s$ excited state of the e_1h_1 ground exciton state. Nevertheless, this agreement does not allow us to determine precisely the valence-band offset α since the calculated $E_{E_1H_1}$ direct gap is not very sensitive to the value of α; we will discuss this problem in the next section.

VI. DETERMINATION OF THE BAND OFFSET

The experimental determination of the valence- and the conduction-band offsets is a difficult task mainly because two major physical problems appear when we deal with this issue. Firstly, the experimental data known from the two bulk materials give only the difference ΔE_g of the gaps which is the *sum* of the valence- and conduction-band offsets. Here, the mixed-type nature of the $CdTe/Cd_{1-x}Zn_xTe$ system offers a unique opportunity to measure the valence-band offset by the energy difference between the e_1h_1 (direct) and e_1l_1 (indirect) transitions, after correction for strain and exciton binding energies. With this last point, we meet the second difficulty, that is, the exciton binding energy, an additional unknown of the problem, which cannot be neglected in this II-VI system ($E_b=11$ meV in the bulk).

The alternative is to compare the calculated optical gap with the gap obtained knowing the experimental ($2s$-$1s$) energy difference. This has been possible for the case of the heavy-hole exciton as shown in Sec. V but, unfortunately, the calculated heavy-hole gap ($E_{E_1H_1}$) is not very sensitive to the parameter α since it involves a direct transition; therefore the experimental data concerning the heavy-hole transition do not allow a precise determination of the valence-band offset. Nevertheless, the mixed nature of our system provides also the indirect light excitonic transition which is very sensitive to the valence-band offset since it is an indirect transition. However, our experimental results have not allowed us to observe experimentally the excited states ($2s$) of the light-hole exciton.

Therefore we have adopted the following procedure in order to get limits for the valence-band offset: for each sample, we calculated the heavy- and light-hole optical gaps ($E_{E_1H_1}$ and $E_{E_1L_1}$) as a function of the parameter α; comparing these values with the experimental values of the heavy- and light-hole excitonic transitions (e_1h_1 and e_1l_1) we obtained the (heavy- and light-hole) excitonic binding energies (E_{bh} and E_{bl}) as a function of α. Because of the indirect nature of the light-hole exciton, its binding energy should be positive and smaller than the heavy-hole exciton binding energy. This condition ap-

plied to a whole set of ten samples shows that the valence-band offset lies between $+0.1$ and -0.1. The assumption that whole band-gap difference lies in the conduction band (in the absence of strain) is therefore accurately justified.

VII. INFLUENCE OF THE STRAIN

The results presented previously have confirmed that the valence-band offset before strain is zero (or very small), i.e., the potentials for heavy and light holes are entirely (or almost entirely) determined by the superlattice's strain state. Therefore, by tailoring the internal strain experienced by each layer of the superlattice (CdTe and $Cd_{1-x}Zn_xTe$), it should be possible to change the superlattice from type I (with the direct, heavy-hole exciton at lower energy) to type II (where the indirect light-hole transition lies lowest). This has been achieved, specifically for structures with (65 Å)/(65 Å) periods, by growing superlattices on a CdTe buffer layer instead of $Cd_{1-x}Zn_xTe$ ($x \approx 0.04$); changing the support's lattice parameter changes which one of the superlattice layers (CdTe or $Cd_{1-x}Zn_xTe$) experiences the most strain.

Figure 6 presents typical spectra for two such samples having different strain states. The first one, S4 [Figs. 6(a)–6(c)] consists of 70 periods grown directly on a $Cd_{1-x}Zn_xTe$ ($x \approx 0.04$) substrate. The second sample, S5 [Figs. 6(d)–6(f)] grown on a 2-μm-thick CdTe buffer layer, was limited to 10 periods since the critical thickness of the whole superlattice is only ≈ 2000 Å in this case.

For both samples, the transition of the intrinsic, heavy-hole exciton e_1h_1 is clearly identified: it corresponds to the strongest feature in the reflectivity spectra. For sample S4, the e_1l_1 transition is observed 4 meV above the e_1h_1 transition, as confirmed by the optical-pumping experiment of Fig. 6(c) (again a positive or negative polarization signal corresponds to heavy- or light-hole character, respectively).

For the sample grown on a CdTe buffer layer (S5), an important change is observed in the optical spectra, as shown in Figs. 6(d)–6(f): the relative energy position of intrinsic lines e_1h_1 and e_1l_1 is reversed. In the reflectivity spectrum [Fig. 6(e)], the strongest feature, which we attribute to the direct transition e_1h_1, is now situated at higher energy than the weaker feature, attributed to the indirect transition e_1l_1. We now compare the luminescence and reflectivity spectra with a polarized photoluminescence spectrum [Fig. 6(f)]. In this case, one excites the sample with circularly polarized light at an energy higher than the energy gap of the barriers (i.e., in the continuum); therefore, if one analyzes the circular polarization of the emission $[I(\sigma_+)-I(\sigma_-)]$, it should be positive or negative in the case of a heavy-hole or light-hole transition, respectively. The low-energy part of the spectrum is characterized by two lines (1595.2 meV with a positive sign and 1598.2 meV with a negative signal) that correspond to the free, heavy and light-hole excitons split off by the residual strain of the CdTe buffer layer (it was previously shown that a thick CdTe layer grown on a $Cd_{0.96}Zn_{0.04}Te$ substrate never relaxes completely[24]). Since this residual strain is a compression—the CdTe layer is grown on a $Cd_{0.96}Zn_{0.04}Te$ substrate—the heavy-hole exciton should indeed lie at a lower energy than the light-hole exciton. Recording the signal related to the

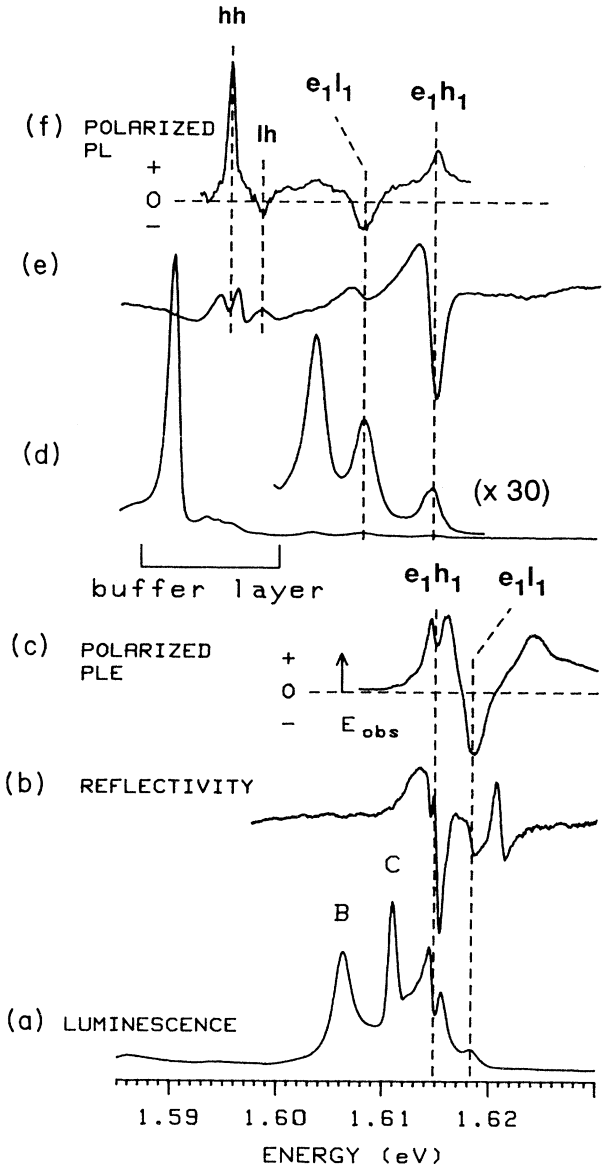

FIG. 6. Photoluminescence [(a) and (d)], reflectivity [(b) and (e)], and polarization spectra detected at energy E_{obs} [(c) and (f)] of a type-I and type-II superlattice ($T = 1.8$ K). Spectra (a)–(c) are for type-I sample S4 [70 (65 Å)/(65 Å) periods grown on a $Cd_{1-x}Zn_xTe$ ($x \approx 0.04$) substrate]; the indirect light-hole exciton line e_1l_1 identified by the polarized PLE spectrum (c) lies higher than the direct heavy-hole exciton structure e_1h_1. Spectra (d)–(f) are for type-II sample S5 [ten (65 Å)/(65 Å) periods grown on a CdTe buffer layer]; the indirect light-hole exciton now lies lower than the direct heavy-hole exciton as shown in the polarized PL spectrum. The strong CdTe exciton emission at 1.59 eV shows efficient energy transfer to the buffer layer; the splitting between the heavy- (*hh*) and light-hole (*lh*) exciton lines that appears clearly in the polarized PL (*f*) is a direct measurement of the residual strain present in the CdTe buffer layer.

CdTe buffer layer provides therefore an unambiguous means to be sure of the sign of the circular polarization. Consequently, the light- and heavy-hole character of the superlattice's transitions at higher energy (1607.9 and 1614.5 meV) is clearly demonstrated by their negative and positive polarizations, respectively [Fig. 6(f)]. The photoluminescence spectrum [Fig. 6(d)] shows another line at 1604 meV that does not correspond to any feature in the reflectivity spectrum or in the polarized photoluminescence spectrum. We therefore associate this line with an extrinsic transition, presumably excitons trapped on impurities or interface defects.

The experimental positions of the heavy- and light-hole exciton transitions are plotted in Fig. 7 for the samples of Fig. 6, as well as for a (65 Å)/(65 Å), CdTe/$Cd_{1-x}Zn_xTe$ ($x \approx 0.08$) superlattice (S6) grown on a $Cd_{1-x}Zn_xTe$ ($x \approx 0.08$) buffer, and a (65 Å)/(65 Å) CdTe/$Cd_{1-x}Zn_xTe$ ($x \approx 0.08$) superlattice (S7) grown on a CdTe substrate. These data are compared with the calculated direct gap $E_{E_1H_1}$ and indirect gap $E_{E_1L_1}$, plotted versus the average strain $\epsilon^{\parallel}$ in the SLS, i.e., as a function of the Zn composition in the buffer layer that imposes the in-plane lattice parameter

We emphasize that the zinc concentration and the

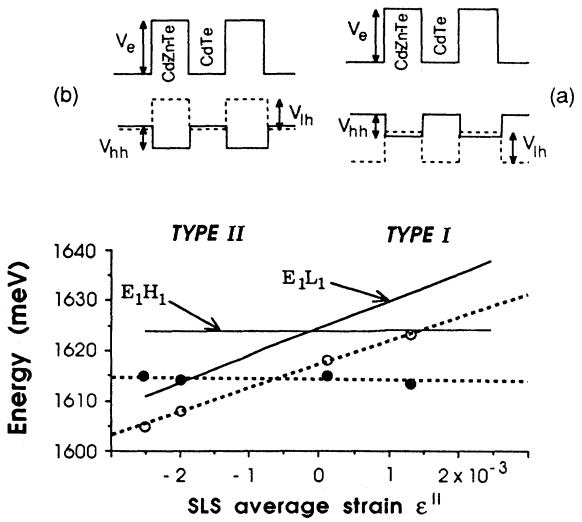

FIG. 7. Influence of $\epsilon^{\parallel}$, the superlattice's average in-plane strain, on the calculated gaps $E_{E_1H_1}$ and $E_{E_1L_1}$ for period (65 Å)/(65 Å) (solid lines) and on the experimental excitonic energies $E_{e_1h_1}$ (●) and $E_{e_1l_1}$ (○) for samples S7, S5, S4, S6 grown respectively on CdTe substrate ($\epsilon^{\parallel} = -2.5 \times 10^{-3}$), CdTe buffer ($\epsilon^{\parallel} = -2.0 \times 10^{-3}$), $Cd_{0.96}Zn_{0.04}Te$ substrate ($\epsilon^{\parallel} = 1.0 \times 10^{-4}$), and $Cd_{0.92}Zn_{0.08}Te$ buffer ($\epsilon^{\parallel} = 1.3 \times 10^{-3}$). The dotted lines drawn through the experimental points are only guides for the eye. The strain $\epsilon^{\parallel} = (a_{\text{free-standing}} - a_{\text{buffer}})/a_{\text{buffer}}$, where $a_{\text{free-standing}}$ is the in-plane lattice parameter of the hypothetical free-standing superlattice and a_{buffer} is the buffer's lattice parameter. The passage from a type-I to a type-II superlattice is illustrated by insets [(a) SL grown on $Cd_{1-x}Zn_xTe$ and (b) SL grown on CdTe], which show schematically the relative positions of the confinement potentials for electrons (V_e), heavy holes (V_{hh}), and light holes (V_{lh}).

width of the barrier and the well layers are the same for the four samples illustrated in Fig. 7. Therefore the depth and widths of the confinement potential V_{hh} for heavy holes and V_{lh} for light holes are practically unchanged when one varies the buffer, see insets (a) and (b) of Fig. 7: the differences in the elastic constants and deformation potentials between CdTe and $Cd_{1-x}Zn_xTe$ ($x \approx 0.08$) are such that the confinement potential V_{hh} and V_{lh} are constant within an accuracy of $\approx 1\%$; varying the buffer only shifts the heavy- and light-hole potentials as a whole relative to each other. Then the inversion of the optical type in the superlattices of Fig. 6 is *entirely due to the strain changes.* This contrasts with the $Ga_{1-x}In_xAs/InP$ SLS system, where the observed change of type is due to the net effect of three different contributions (alloy composition, strain, and quantum size effects).[3]

For period (65 Å)/(65 Å), the crossover of the $E_{E_1H_1}$ and $E_{E_1L_1}$ gaps, i.e., the point where the light-hole band edge (in $Cd_{1-x}Zn_xTe$) and the heavy-hole band edge (in CdTe) are at the same energy, occurs for $\epsilon^{\parallel}$ very close to zero (case of 4 mol % Zn substrate), see Fig. 7, i.e., when the strain is almost equally shared between the two kinds of layers. At this point the e_1h_1 and e_1l_1 excitons have different energies (Fig. 7) because of their binding energy difference: this is why the experimental excitonic gaps cross at a different value of $\epsilon^{\parallel}$ (see Fig. 7).

We want to point out that such a type-II spectroscopic signature has been obtained for CdTe/$Cd_{0.92}Zn_{0.08}Te$ superlattices in different strain states (samples S7 and S5, see Fig. 7) and also for CdTe/$Cd_{1-y}Zn_yTe$ superlattices with different zinc concentrations in the $Cd_{1-y}Zn_yTe$ barriers ($y = 0.6$ and 0.12).

VIII. CONCLUSION

In conclusion, this extended optical study of CdTe/$Cd_{0.92}Zn_{0.08}Te$ superlattices has demonstrated several interesting band-structure effects. First, the system CdTe/$Cd_{1-x}Zn_xTe$ is characterized by a very small chemical valence-band offset ($-0.1 < \alpha < 0.1$) in agreement with Tersoff's theoretical predictions[25] that give a valence-band offset close to zero at the CdTe/ZnTe interface. Second, because the valence-band alignment is strongly influenced by the strain, the biaxial stress experienced by each layer of the superlattice determines the potential alignment for the holes. We show then the mixed nature of the superlattice band-gap configuration: electrons and heavy holes are confined in the CdTe layers (type I or direct excitons), whereas light holes are confined in the $Cd_{1-x}Zn_xTe$ layers (type II or indirect excitons).

Moreover, our set of samples has allowed us to study the influence of two structural parameters on the SLS band structure: the period and the deformation.

The variation of the experimental light- and heavy-hole exciton energies compared with the calculated gaps was obtained as a function of the period, for a given strain state of the SLS. This leads to the variation of the binding energy of a direct exciton (the heavy-hole exciton)

compared to an indirect one (the light-hole exciton). We found that the heavy-hole exciton binding energy remains approximately constant though the whole range of periods (120–400 Å), which is clearly confirmed by the observation and identification of the $2s$ excited state of the heavy-hole e_1h_1 exciton. By contrast, the light-hole exciton binding energy decreases significantly when the period increases, which is consistent with the indirect nature of this exciton.

Finally, we have demonstrated that the valence-band configuration can be tailored by the internal strain imposed by the substrate or the buffer layer: the passage from a type-I superlattice (the direct, heavy-hole exciton being at lower energy) to a type-II superlattice (with the indirect light-hole exciton transition lowest) was obtained. This was achieved just by changing the internal deformation of the superlattice, namely by growing a set of SLS's on buffer layers of different zinc concentrations; by varying the buffer layer composition, i.e., by imposing the largest strain either in the CdTe or in the $Cd_{1-x}Zn_xTe$ layers, the superlattice's ground state has been made to be either type I or type II.

The simultaneous observation of direct and indirect exciton transition in $CdTe/Cd_{1-x}Zn_xTe$ superlattices makes this system very attractive to study the influence of an electric field and the basic electro-optic properties of II-VI heterostructures.

ACKNOWLEDGMENTS

We should like to acknowledge P. Gentile, B. Gilles, G. Lentz, and A. Ponchet for their assistance in growing and characterizing the samples and R. T. Cox, Le Si Dang, and J. L. Pautrat for helpful discussions. This work was supported by the Commissariat à l'Energie Atomique–Centre National de la Recherche Scientifique joint group for II-VI semiconductor microstructures. The Laboratoire de Spectrométrie Physique is Unité associée au Centre National de la Recherche Scientifique No. 8.

[1]See the review by G. C. Osbourne, P. L. Gourley, I. J. Fritz, R. M. Biefield, L. R. Dawson, and T. E. Zipperian, Semicond. Semimetals **24**, 459 (1987).

[2]J. Y. Marzin and J. M. Gerard, Superlattices Microstruct. **5**, 51 (1989).

[3]D. Gershoni and H. Temkin, J. Lumin. **44**, 381 (1989).

[4]J. Y. Marzin, M. N. Charasse, and B. Sermage, Phys. Rev. B **31**, 8298 (1985).

[5]In this paper, the words "direct" and "indirect" apply to real space always, all the observed transitions being direct in **k** space in these materials.

[6]G. Monfroy, S. Sivananthan, Y. Chu, J. P. Faurie, R. D. Knox, and J. L. Standenmann, Appl. Phys. Lett. **49**, 153 (1986).

[7]H. Mathieu, A. Chatt, J. Allegre, and J. P. Faurie, Phys. Rev. B **41**, 6082 (1990), and references cited therein.

[8]J. Cibert, Y. Gobil, Le Si Dang, S. Tatarenko, G. Feuillet, P. H. Jouneau, and K. Saminadayar, Appl. Phys. Lett. **56**, 292 (1990).

[9]For the purposes of cross reference to other previously published work on these materials, the samples designated S1, S2, S3, S4, S5, S6, and S7 in the present paper correspond to Z339, Z397, Z296, Z327, Z354, Z373, and Z399 respectively, in the crystal-growers' notation.

[10]G. Lentz, A. Ponchet, N. Magnea, and H. Mariettte, Appl. Phys. Lett. **55**, 2733 (1989); A. Ponchet, G. Lentz, H. Tuffigo, N. Magnea, H. Mariette, and P. Gentile, J. Appl. Phys. **68**, 6229 (1990).

[11]R. Zachai, K. Eberl, G. Abstreiter, E. Kasper, and H. Kibbel, Phys. Rev. Lett. **64**, 1055 (1990), and references cited therein.

[12]H. Tuffigo, R. T. Cox, F. Dal'Bo, G. Lentz, N. Magnea, H. Mariette, and C. Grattepain, Superlattices Microstruct. **5**, 83 (1989).

[13]Y. Merle d'Aubigné, Le Si Dang, F. Dal'Bo, G. Lentz, N. Magnea, and H. Mariette, Superlattices Microstruct. **5**, 367 (1989).

[14]E. Cohen, R. A. Street, and A. Muranevich, Phys. Rev. B **28**, 7115 (1983).

[15]C. Weisbuch, R. C. Miller, R. Dingle, A. C. Gossard, and W. Wiegman, Solid State Commun. **37**, 219 (1981).

[16]Ch. Neuman, A. Nöthe, and N. O. Lipari, Phys. Rev. B **37**, 922 (1988).

[17]H. Mariette, F. Dal'Bo, N. Magnea, G. Lentz, and H. Tuffigo, Phys. Rev. B **38**, 12 443 (1988).

[18]M. Zigone, H. Roux-Buisson, H. Tuffigo, N. Magnea, and H. Mariette, Semicond. Sci. Technol. (to be published).

[19]D. L. Camphausen, G. A. N. Connel, and W. Paul, Phys. Rev. Lett. **26**, 184 (1971).

[20]Y. Merle d'Aubigné, H. Mariette, N. Magnea, H. Tuffigo, R. T. Cox, G. Lentz, Le Si Dang, J. L. Pautrat, and A. Wasiela, J. Cryst. Growth. **101**, 650 (1990).

[21]H. Tuffigo, R. T. Cox, N. Magnea, Y. Merle d'Aubigné, A. Million, Phys. Rev. B **37**, 4310 (1988).

[22]H. Tuffigo, B. Lavigne, R. T. Cox, G. Lentz, N. Magnea, and H. Mariette, Surf. Sci. **229**, 480 (1990).

[23]N. Hung-Sik Cho and Paul. R. Prucnal, Phys. Rev. B **36**, 3237 (1987).

[24]F. Dal'Bo, G. Lentz, N. Magnea, H. Mariette, Le Si Dang, and J. L. Pautrat, J. Appl. Phys. **66**, 1338 (1989).

[25]J. Tersoff, Phys. Rev. Lett. **56**, 2755 (1986).